Journal of Materials Chemistry B

Accepted Manuscript

ROYAL SOCIETY OF CHEMISTRY

www.rsc.org/materialsB

Journal of Materials Chemistry B

Dynamic Article Links ►

Cite this: DOI: 10.1039/c0xx00000x

www.rsc.org/xxxxxx

Communication

Effects of fluorine on the structure of fluorohydroxyapatite: a study by XRD, solid-state NMR and Raman spectroscopy

Jinshuai Chen,[a,b‡] Zhiwu Yu,[c‡] Peizhi Zhu,*[a, b] Junfeng Wang,[c] Zhehong Gan,[d] Jie Wei,[e] Yinghui Zhao[f] and Shicheng Wei*[f]

Received (in XXX, XXX) Xth XXXXXXXXX 20XX, Accepted Xth XXXXXXXXX 20XX
DOI: 10.1039/b000000x

For the first time we observed well-resolved Ca(I) and Ca(II) signal changes in fluorohydroxyapatites with different fluorine contents by solid state NMR. The experiment results show that fluorine ions perturbs the chemical environment of Ca(II) ions and OH^- ions more than phosphorous tetrahedrons and Ca(I) ions.

Hydroxyapatite (HA) is the main mineral in teeth and bones within the human body. Tooth Enamel, the hardest and most highly mineralized substance in the human body, contains roughly 96 percent of hydroxyapatite. Fluorine-substituted hydroxyapatite (FHA) is chemically more stable than hydroxyapatite in acid environment.[1] A higher concentration of FHA in tooth enamel decreases tooth dissolution and therefore decreases the incidence of tooth decay. It also has been reported that fluorine-substituted hydroxyapatites support cellular proliferation and colonization and promote bone growth.[2]

Over recent years, fluorohydroxyapatite has been used as bioactive ceramic coatings due to its enhanced biocompatibility as compared to the other ceramic coatings. [3,4] Fluoride-containing bioactive glasses are of particular interest in many fields of dentistry and orthopedics because they are osteoconductive and can combine the benefits of fluorapatite (FA) with the bone-regenerative properties of bioactive glasses. [5-10] In FHA composition, part of the OH^- ions are substituted by F^- ions in order to improve material stability. However, most studies so far have focused on the preparation methods of FHA and its thermal and chemical stability.[11] The effects of different fluorine contents on the structure have seldom been studied systematically. The resistance of fluorohydroxyapatite to acids depends largely on its chemical structure, it is of great interest to determine its structure that prevents the process of erosion.

The hydroxyapatite structure and substitution in hydroxyapatite by different anions and cations including Pb^{2+}, Mg^{2+}, Ti^{4+}, CO_3^{2-}, Cl^- and F^- ions [12-18] have been extensively studied and characterized by X-ray diffraction (XRD)[5-10, 14-16, 23], solid state NMR [12-14, 17-23] and Raman spectroscopy.[18] Molecular dynamic simulations have also been used to investigate the transport of fluorine in fluoraptite and this study found that a sequence of F^- ions moving along the *c*-axis in a concerted mechanism, *via* lattice and interstitial sites.[24] In this study, a series of FHAs with varying fluorine levels ($Ca_{10}(PO_4)_6(OH)_{2-X}F_X$ from x = 0 to 2) were synthesized through the wet precipitation method using $Ca(NO_3)_2{\bullet}4H_2O$ and $(NH_4)_2HPO_4$ as starting materials and NH4F as a source for fluorine incorporation. (see Supplementary Information for materials synthesis and experimental details). The structure of synthesized FHAs were characterized by ^1H, ^{43}Ca, ^{31}P and ^{19}F NMR MAS solid-state NMR, XRD and Raman spectroscopy to examine the effect of fluorine substitution on the hydroxyapatite structure.

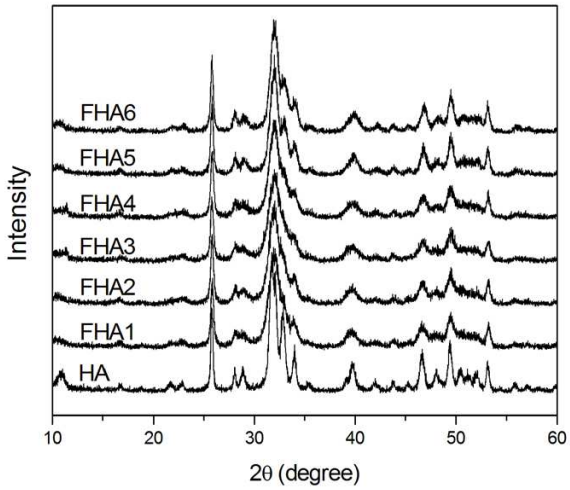

Fig. 1 XRD patterns of fluorohydroxyapatites containing different fluorine levels (HA: 0wt%, FHA1: 0.54wt%, FHA2:0.83wt%, FHA3:1.59wt%, FHA4: 1.93wt%, FHA5: 2.2wt%, FHA6: 2.94wt%).

XRD pattern of fluorohydroxyapatites containing different fluorine levels are shown in Fig. 1. The typical peaks of apatites are at 28.1°, 28.9°, 31.7°, 32.8° and 34.0°, which are corresponding to the (1 0 2), (2 1 0), (2 1 1), (3 0 0), (2 0 2), (3 1 0), (2 2 2), (2 1 3) and (0 0 4) miller's planes, respectively.[23] With the increase of F^- ion content in HA, some small peaks in the range of 45~50° become noisy and

Cite this: DOI: 10.1039/c0xx00000x

www.rsc.org/xxxxxx

Communication

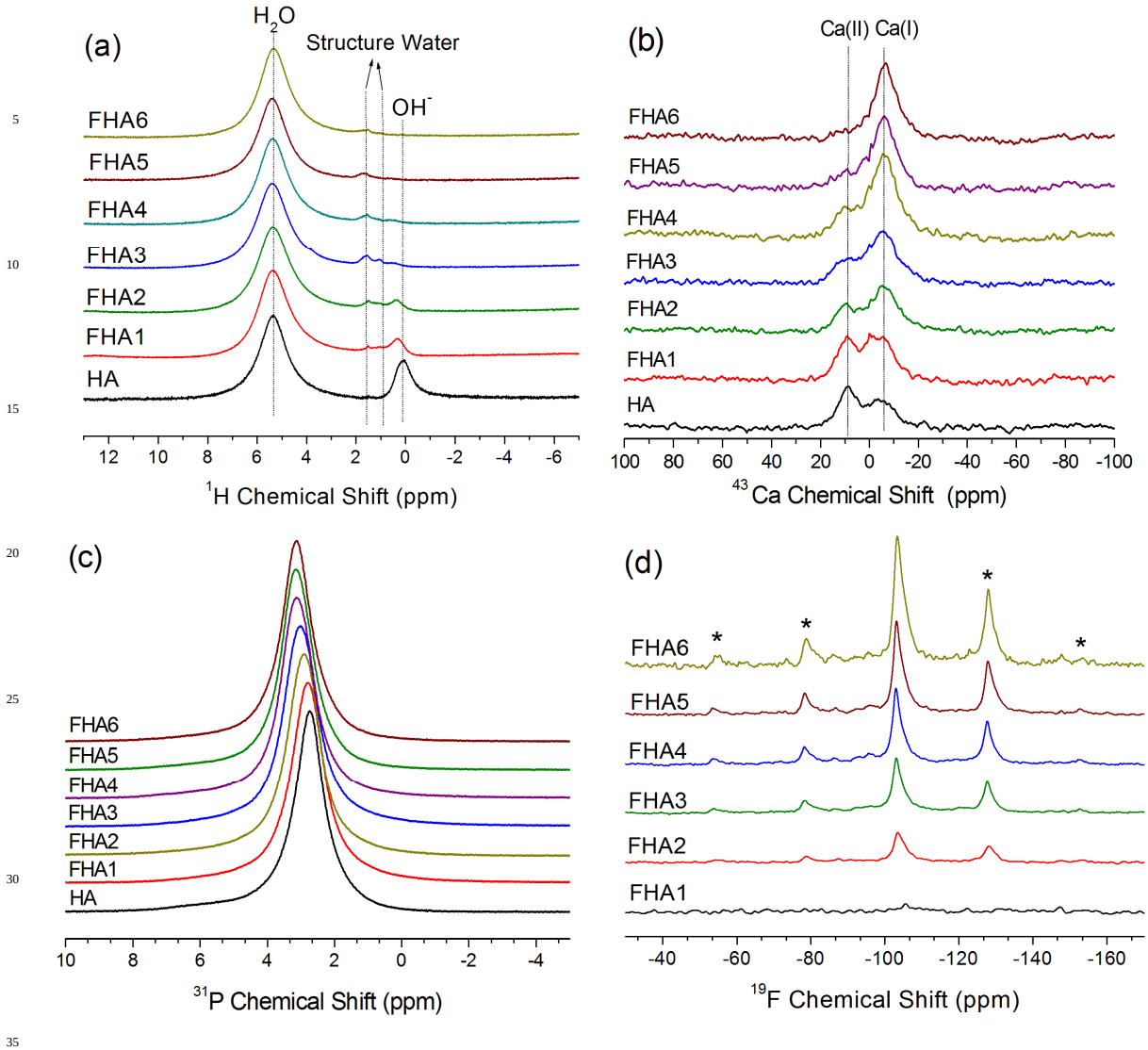

Fig. 2 (a) ^{1}H NMR spectra, (b) ^{43}Ca NMR spectra, (c)^{31}P NMR spectra, and (d) ^{19}F NMR spectra of fluorohydroxyapatites containing different fluorine levels (HA: 0wt%, FHA1: 0.54wt%, FHA2:0.83wt%, FHA3:1.59wt%, FHA4: 1.93wt%, FHA5: 2.2wt%, FHA6: 2.94wt%). The acquisition time for each ^{1}H, ^{43}Ca and ^{31}P spectrum were 5 min, 24 hours and 1 hour, respectively. All ^{1}H and ^{31}P NMR spectra were obtained using a Varian VNMRS 400 MHz solid-state NMR spectrometer and a 6 mm double-resonance MAS probe with a spinning frequency of 8 kHz. All ^{43}Ca spectra were obtained on a 830 MHz solid-state NMR spectrometer using a single-resonance 4 mm MAS probe with a spinning frequency of 10 kHz at room temperature (25 °C). Solid-state ^{19}F NMR experiments were performed on a Bruker 600 MHz NMR spectrometer using a spin echo pulse excitation. A π/2 pulse length of 5.57 μs, a recycle delay of 2 s, a spinning rate of 14 kHz and the echo time set to five rotor period were used for ^{19}F MAS NMR experiments. Asterisks denote spinning sidebands.

disappear, and peaks of (2 1 1), (3 0 0) and (2 0 0) gradually shift to the right-hand side with an increase in F^- ions incorporated within the apatite lattice. The shifts are caused by the decrease in a-axis length of the hexagonal crystals lattice induced by the lower ionic radius of F^- ions.[11]

The ^{1}H MAS NMR spectrum of hydroxyapatite (HA) is shown in Fig.2a. Two main peaks are observed, one peak at 0.3 ppm corresponding to hydroxyl ions and the other at 4.95 ppm coresponding to water molecules on the surface of hydroxyapatite, which agree with previous reports.[20-21] As the fluorine content increases, the chemical shift of OH^- ions in the lattice of apatites gradually shifts upfield and the height of peak decrease due to substitution of F^- ions. With the 0.54% fluorine added to hydroxyapatite lattice shown in the spectrum of FHA1, the signal of hydroxyl ions significantly decreases

and gets broader but a new peak at 1.8 ppm appears, which can be assigned to structure water forming strong bonding with the surface vacancies of crystal lattice of apatite. As the fluorine content increases to 0.83 wt% (FHA2), the signal of hydroxyl continues to decrease and the peak at 1.8 ppm can also be observed. When the fluorine content increases to 1.593 wt% (FHA3), the signal of hydroxyl almost disappears and two peaks at 1 ppm and 1.8 ppm are observed. These two peaks can be all assigned to structure water molecules. As the fluorine content increases to 1.93 wt% (FHA4), the surface water peak at 4.97 ppm and two structure water peaks at 0.8 ppm and 1.8 ppm can be observed. When the fluorine content increases to 2.2 wt% (FHA5) and 2.94 wt% (FHA6), only the surface water peak at 4.97 ppm and structure water peak at 1.8 ppm are observed, indicating OH^- ions have been completely substituted by F^- ions.

Fig.2b shows nature abundance ^{43}Ca NMR spectra of fluorohydroxylapatites containing different fluorine levels. The spectrum of HA shows Ca (I) and Ca (II) peaks of hydroxyapatite at 9.6 ppm and -5.6 ppm, respectively.[12,17] As the fluorine content increases, Ca (II) peak shifts downfield, while the Ca (I) position unchanged, indicating that the increased fluorine content significantly changes the chemical environment of Ca (II) ions by reducing the Ca (II)-O bond length but the impact on Ca (I) is minimal. NMR chemical shift is sensitive to the shielding of electrons which usually causes a downfield shift in low electron density environments. It follows that highly fluorine-level apatites have a lower chemical shift, as confirmed in this study. These results are consistent with XRD studies. The Ca(I) ion is coordinated to nine oxygen atoms in the arrangement of tricaped trigonal prism and Ca (I) polyhedron shows little response to incorporation of different anion ions. However, in Ca(II) ployhedron, Ca(II) ion bonds to six oxygen atoms and one column anion. Therefore, the major structure substitution of OH^- ions by F^- ions will impact Ca(II) ions.

The ^{31}P MAS NMR spectra of the fluorohydroxyapatites with various fluorine contents are shown in Fig.2c. The ^{31}P NMR spectrum of all samples exhibits a single well-resolved resonance at 2.8 ppm. This resonance is shifted upfield to higher ppm values as fluorine contents increase from 0wt% to 1.59wt%, then remain at same 3.4 ppm from 1.93 wt% to 2.94 wt%. The phosphorus signal become progressively narrow as fluorine contents increase, indicating the increased crystallinity by the incorporation of fluorine into the HA lattice. Phosphorous atoms exist in apatite in tetrahedral coordination with four oxygen atoms. These rigid tetrahedra show a bit chemical environment change with fluorine substitution from 0wt% to 1.59wt%, but almost no chemical shift change from 1.93 wt% to 2.94 wt% due to the high structural similarity of the phosphorous atoms in these fluorine substituted hydroxyapatites.

The ^{19}F MAS NMR spectra of FHAs containing different fluorine levels are shown in Fig.2d. The ^{31}F NMR spectra exhibit one peak at around -103ppm and a few sidebands, which is similar to those previous results for fluorapatites.[23] The height of fluorine signal increases with fluorine levels, showing that OH^- ions in apatite lattice are gradually substituted by F^- ions. With the 0.54% fluorine added to hydroxyapatite lattice shown in the spectrum of FHA1, the signal of F^- ions is very weak because of the low fluorine content. As the fluorine content increases, F^- ions in apatite lattice become less shield and the fluorine chemical shift moves downfield.

Fig 3a shows the Raman spectra of all seven apatite samples with different fluorine content. All spectra have a strong PO_4^{3-} band at ~960 cm−1. As fluorine content increases, the PO_4^{3-} band associated with the P–O stretch shifts upfield, which suggests a progressive shortening of the P–O bond due to increasing content of fluorine ions. The replacement of OH^- ions by a smaller F^- ions increases electrostatic attraction between the oxygen atoms in the phosphate tetrahedra, which then produces a shortening of the P–O bonds and an increase in vibrational frequency. The Full Width at the Half-Height (FWHH) of the phosphate symmetric stretch at 960 cm^{-1} as a measure of crystallinity increases with fluorine levels. [18,19] Fig. 3b shows the decrease in intensity of the O–H stretch at about 3580 cm^{-1} (normalized to the intensity of the 960 cm^{-1} peak) with increasing fluorine content. The peak remains at about the same position but shows broadening and development of a shoulder at about 3545 cm^{-1} side of the major O–H band at 3580 cm^{-1}. As the fluorine content increases to 0.83 wt% (FHA3), two peak at 3545 cm^{-1} and 3580 cm^{-1} can be observed. While the fluorine content increases to 1.593 wt% (FHA4), the band at 3580 cm^{-1} of O–H continues to decrease and its signal becomes weaker than the band at 3545 cm^{-1}. As the fluorine content increases to 2.2 wt% (FHA5), the O–H band at 3580 cm^{-1} disappears and only one weak band at 3545 cm^{-1} can be observed. For FHA6 sample, no peak can be observed, indicating that hydroxyl ions have been completely substituted by F^- ions, which agrees well with ^1H NMR results shown by Fig.2a. Therefore, extensive substitution of O–H group by F^- ions may sufficiently alter the environment of the channel sites to cause a shift in the vibrational frequency of some O–H groups, leading to the development of a shoulder band at high fluorine concentrations. Alternatively, at high fluorine content, fluorine may begin to substitute preferentially into the channel site.[23,24]

HA, FHAs and FA are widely used as biomaterials in bone tissue engineering and dental caries treatment. The chemical composition and surface characteristics of the biomaterials used as bone implants are important factors in affecting the cells at the interface between the material and the surrounding tissues. [3,4] The substitution of OH^- ions by F^- ions and content of F^- ions in HA lattice can be controlled in the synthesis process (see materials synthesis in Supplementary Information). When all OH^- ions have been replaced by F^- ions, fluorapaptite is formed. The addition of F^- ions to HA lattice caused the increase of the thermal and chemical stability of the HA. [11] In the crystal structure of HA, the atoms

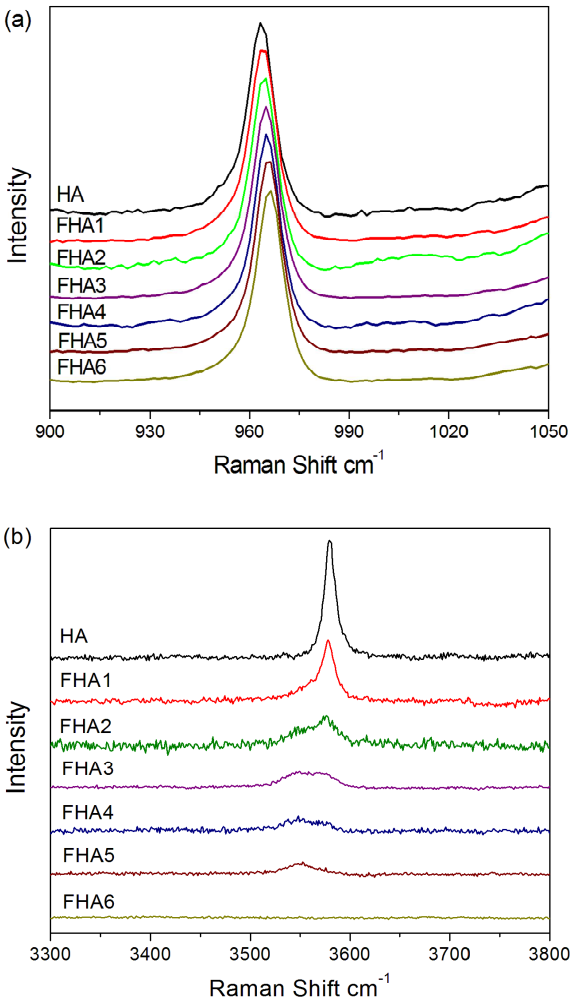

Fig.3 Raman spectra of fluorohydroxyapatites containing different fluorine levels (HA: 0wt%, FHA1: 0.54wt%, FHA2: 0.83wt%, FHA3: 1.59wt%, FHA4: 1.93wt%, FHA5: 2.2wt%, FHA6: 2.94wt%) in the range of (a) 900~1050 cm^{-1} and (b)3100~3800 cm^{-1}.

of OH^- ions sit in the atomic interstices neighbouring to the oxygen atoms and O-H group are oriented randomly, which brings a certain degree of disorder to the crystal structure of HA. [25] When the OH^- ions are partially substituted by the F^- ions, the existing hydrogen atoms of the OH groups are bound to the nearby F^- ions and become more ordered. In the crystal lattice of FHAs, OH^- ions and F^- ions are only surrounded by Ca (II) ions. When OH^- ion are gradually substitute by F^- ions, the higher affinity and smaller size of the fluorine atoms with respect to the oxygen atoms, and the improved bonding between F^- ions and Ca(II) ions produce an increasingly compact and ordered apatite structure and also change the chemical environment of HA surface, which are shown by ssNMR results in Fig 2.

In summary, a series of fluorohydroxyapatites were synthesised and characterized to evaluate the effects of fluorine on the structure of hydroxyapatite. For the first time we observed the well-resolved Ca(I) and Ca(II) signal change in fluorohydroxylapatite with different fluorine contents at nature abundance. Compared with small variations of ^{31}P NMR chemical shift induced by incorporation of fluorine, the significant ^{43}Ca NMR signal change of Ca(II) ions and ^{1}H NMR signal change of OH^- ions indicate that the fluorine perturbs the chemical environment of Ca(II) ions and OH^- ions more than phosphorous atoms. Fluorohroxyapatite has extensive application in teeth and bone materials. The combination of ^{1}H, ^{43}Ca, ^{31}P and ^{19}F NMR MAS solid-state NMR, XRD and Raman spectroscopy can probe the structure of fluorohydoxyapatite at atomic level. Especially the solid state ^{43}Ca NMR can selectively and sensitively detect the chemical environments of calcium ion, which could be a powerful tool in the field of biomaterials, bioglass ceramics and geological materials.

Acknowledgment

This work was supported by Jiangsu Province for specially appointed professorship to Dr. P.Z. Zhu, research funds from Yangzhou University and the support from Testing Center of Yangzhou University. Prof. S.C. Wei thanks the support from State Key Development Program for Basic Research of China (Grant 2007CB936103) and Peking University's 985 Grant. This work was also supported by the National High Magnetic Field Laboratory through the National Science Foundation Cooperative Agreement (DMR-0084173) and by the State of Florida.

Notes and references

[‡]*These authors contribute equally to this work.*
[a]*School of Chemistry and Chemical Engineering, Yangzhou University, Jiangsu, P.R. China, 225009,Email: pzzhu@yzu.edu.cn*
[b]*Jiangsu Co-innovation Center for Prevention and Control of Important Animal Infectious Diseases and Zoonoses, Yandzhou, 225009*
[c]*High Magnetic Field Laboratory, Hefei Institutes of Physical Science, Chinese Academy of Sciences, 350 Shushanhu Road, Hefei 230031, Anhui Province, China*
[d]*Center of Interdisciplinary Magnetic Resonance, National High Magnetic Field Laboratory, Tallahassee, FL, 32310, USA*
[e]*Key Laboratory for Ultrafine Materials of Ministry of Education, East China University of Science and Technology, Shanghai, P.R. China, 200237*
[f]*Department of Oral and Maxillofacial Surgery, Laboratory of Interdisciplinary Studies, School and Hospital of Stomatology, Peking University, Beijing 100081, P.R. China, Email: sc-wei@pku.edu.cn*
**corresponding author*

Electronic Supplementary Information (ESI) available: Materials synthesis, and experimental details including X-Ray diffraction (XRD) Measurements, X-ray Photoelectron Spectroscopy (XPS) Measurements, Solid State NMR Spectroscopy, Raman Measurements.
See DOI: 10.1039/b000000x/

1. M. Okazaki, Y. Miake, H. Tohda, T. Yanagisawa, T. Matsumoto and J. Takahashi, *Biomaterials*, 1999, **20**, 1421–1426.
2. J. Harrison, A. J. Melville, J. S. Forsythe, B. C. Muddle, A. O. Trounson and K. A. Gross, *Biomaterials*, 2004, **25**, 4977–4986.
3. D. S. Brauer, N. Karpukhina, R. V. Law, R. G. Hill, *J. Mater. Chem.*, 2009, **19**, 5629–5636.
4. D. Campocciaa, C.R. Arciolaa, M. Cervellatia, M.C. Maltarelloc, L. Montanaro, *Biomaterials*, 2003, **24**, 587–596.
5. L. Montanaro, C.R. Arciola, D. Campoccia, M. Cervellati. *Biomaterials*, 2002, **23**, 3651–3659.
6. D. S. Brauer, M. N. Anjum, M. Mneimne, R. M. Wilson, H. Doweidar and R.G. Hill, *J. Non-Cryst. Solids.*, 2012, **358**, 1438-1442.

7. E. Lynch, D. S. Brauer,; N. Karpukhina, D. G. Gillam and R. G. Hill, *Dent. Mater*., 2012, **28**, 168-178.
8. A. Pedone, T. Charpentier and M. C. Menziani, *J. Mater. Chem.*,2012, **22**, 12599– 12608.
9. I. Kansal, A. Goel, D. U. Tulyaganov, L. F. Santos and J. M. F. Ferreira, *J. Mater. Chem.*, 2011, **21**, 8074-8084.
10. M. Mneimne, R. G. Hill, A. J. Bushby and D. S. Brauer, *Acta. Biomater*., 2011, **7**, 1827-1834.
11. Y. M. Chen and X. G. Miao, *Biomaterials*, 2005, **26**,1205-1210.
12. H. Pizzala, S. Caldarelli, J. Eon, A. M. Rossi, D. Laurencin and M. E. Smith, *J. Am. Chem. Soc.*, 2009, **131**, 5145-5152.
13. D. Laurencin, N. Almora-Barrios, N. H. de Leeuw, C. Gervais, C. Bonhomme, F. Mauri, W. Chrzanowski, J. C. Knowles, R. J. Newport, A. Wong, Z. Gan and M. E. Smith, *Biomaterials*, 2011, **32**, 1826-1837.
14. A.A. Chaudhry, J. Goodall, M. Vickers, J. K. Cockcroft, I. Rehman, J. C. Knowles and J.A. Darr, *J. Mater. Chem.* 2008, **18**, 5900–5908.
15. P. N. Gunawidjaja,; I.Izquierdo-Barba, R. Mathew, K. Jansson, A. García , J. Grins, D. Arcos, M. Vallet-Regí and M. Edén, *J. Mater. Chem.*, 2012, **22**, 7214-7223.
16. C. J. L. Silwood, I. Abrahams, D. C. Apperley, N. P. Lockyer, E. Lynch, M. Motevalli , R. M. Nix and M. Grootveld, *J. Mater. Chem.*, 2005, **15**, 1626-1636.
17. J. Xu, P. Zhu, Z. Gan, N. Sahar, M. M. J. Tecklenburg, M. D. Morris, D. H. Kohn and A. Ramamoorthy, *J. Am. Chem. Soc.*, 2010, **132**, 11504–11509.
18. M.D. O'Donnell, R.G. Hill, R.V. Law and S. Fong, *J. Eur. Ceram. Soc.*, 2009, **29**, 377–384.
19. J-D. P. McElderry, P. Zhu, K.H. Mroue et. al., *J. Solid. State. Chem.*, 2013, **206**, 192–198.
20. E. E. Wilson, A. Awonusi, M. D. Morris, D. H. Kohn, M. M. J. Tecklenburg and L. W. Beck, *Biophys. J*., 2006, **90**, 3722-3731.
21. G. Cho, Y. Wu and J. L. Ackerman, *Science*, 2003, **300**, 1123– 1127.
22. D. Laurencin, A.Wong, J. V. Hanna, R. Dupree, M. E. Smith, *J. Am. Chem. Soc*., 2008, **130**, 2412-2413.
23. F. M. Mccubbin, H. E. Mason, H. Park, B. L. Phillips, J. B. Parise, H. Nekvasil and D. H. Lindsley, *Am. Mineral.*, 2008, **93**, 210– 216.
24. E. E. Jay, M. J. D. Rushton and R. W. Grimes, *J. Mater. Chem.*, 2012, **22**, 6097-6103.
25. H. Eslami, M. Solati-Hashjin, and M. Tahriri, *Adv.Appl.Ceram*., 2010, **109**, 200–212.